

# Introduction

In this note we try to derive the form of the measured signal, as well as investigate its properties under the assumption of a finite particle phase and oscillation frequency distributions.

## 1 Projection of polarization

The polarization of the beam is the sum of the spins of the particles in it. We measure the projection of the polarization on the  $y$ -axis:

$$\begin{aligned}\vec{P} &= \sum_{i=1}^{n_b} \vec{s}_i, \\ \pi_{\hat{y}} \vec{s} &\equiv \hat{y} \cdot \vec{s} = |\vec{s}| \cos \Theta, \\ \pi_{\hat{y}} \vec{P}(t) &= \sum_i \pi_{\hat{y}} \vec{s}_i = |\vec{s}| \sum_i \cos \Theta_i(t), \\ \Theta_i(t) &= \omega_i \cdot t + \phi_i.\end{aligned}\tag{1}$$

The signal at time  $t$  is a sum of random variables, and hence has expectation

$$\begin{aligned}\mathbb{E} [\pi_{\hat{y}} \vec{P}(t)] &= |\vec{s}| \sum_i \mathbb{E} [\cos \Theta_i(t)] = |\vec{s}| \sum_i \int_{-\infty}^{\infty} \cos x \cdot f_{\Theta_i(t)}(x) dx \\ &= |\vec{s}| \sum_i \int_{-1}^{+1} f_{\Theta_i(t)}(\arcsin y) dy.\end{aligned}$$

### 1.1 Distribution of $\Theta_i(t)$

If the distribution of  $\omega_i$  is  $f_{\omega}(x)$ , then that of  $\omega_i t$  is  $f_{\omega t}(x) = \frac{1}{t} f_{\omega}(\frac{x}{t})$ . The distribution of  $\Theta_i(t)$  is the convolution

$$(f_{\omega t} * f_{\phi})(\theta) \triangleq \int_{-\infty}^{\infty} f_{\omega t}(\theta - y) f_{\phi}(y) dy = \frac{1}{t} \int_{-\infty}^{\infty} f_{\omega} \left( \frac{\theta - y}{t} \right) f_{\phi}(y) dy.$$

Assuming  $\omega_i = \omega_0 + G\Delta\gamma_i^2$  and  $f_{\Delta\gamma}(y) = \mathcal{N}(0, \sigma_{\Delta\gamma}^2)(y)$ ,

$$f_{\Delta\gamma^2}(y) = \begin{cases} \frac{1}{\sigma_{\Delta\gamma}^2} \cdot \chi_1^2 \left( \frac{y}{\sigma_{\Delta\gamma}^2} \right), & y \geq 0, \\ 0, & y < 0; \end{cases}$$

and

$$f_{\omega}(x) = \begin{cases} \frac{1}{G\sigma_{\Delta\gamma}^2} \chi_1^2 \left( \frac{x - \omega_0}{G\sigma_{\Delta\gamma}^2} \right), & x \geq \omega_0, \\ 0 & x < \omega_0. \end{cases}\tag{2}$$

$$f_{\omega}(x) = \begin{cases} A(a, \omega_0) \cdot \frac{\exp(-\frac{1}{2}ax)}{\sqrt{x - \omega_0}}, & x \geq \omega_0, \\ 0, & x < \omega_0, \end{cases}$$

with

$$A(a, \omega_0) \equiv \frac{a \exp(\frac{1}{2}a\omega_0)}{\sqrt{2\pi a}}, \quad a \equiv \frac{1}{G\sigma_{\Delta\gamma}^2}.\tag{3}$$

$$f_{\omega} \left( \frac{\theta - y}{t} \right) = \begin{cases} A(a, \omega_0) \cdot B(\theta, t) \cdot \frac{\exp(\frac{ay}{2t})}{\sqrt{\Delta\theta(t) - y}}, & y \leq \Delta\theta(t), \\ 0, & y > \Delta\theta(t), \end{cases}$$

where

$$B(\theta, t) \equiv \sqrt{t} \exp \left( -\frac{a\theta}{2t} \right), \quad \Delta\theta(t) \equiv \theta - \omega_0 t.\tag{4}$$

We'll assume a normally distributed  $\phi_i \sim \mathcal{N}(\phi_0, \sigma_\phi)$ .

Hence,

$$f_{\Theta(t)}(\theta) = (f_{\omega t} * f_\phi)(\theta) = \frac{1}{t} A(a, \omega_0) C(\phi_0, \sigma_\phi) \cdot B(\theta, t) D(\theta, \omega_0 t),$$

where

$$D(\theta, \omega_0 t) \equiv \int_{-\infty}^{\Delta\theta(t)} \frac{\exp(\xi y - y^2/\sigma_\phi^2)}{\sqrt{\Delta\theta(t) - y}} dy, \quad (5)$$

$$C(\phi_0, \sigma_\phi) \equiv \exp\left(\frac{\phi_0^2}{\sigma_\phi^2}\right), \quad \xi \equiv \frac{a\sigma_\phi^2 + 4t\phi_0}{2t\sigma_\phi^2}. \quad (6)$$

## 2 Simulation

### 2.1 $G$

From eq. (2),  $\text{var}\left[\frac{\omega}{G\sigma_{\Delta\gamma}^2}\right] = (G\sigma_{\Delta\gamma}^2)^{-2} \cdot \text{var}[\omega] = 2$ , hence  $\text{var}[\omega] = 2(G\sigma_{\Delta\gamma}^2)^2$ .

$\text{var}[\omega T] = T^2 \cdot \text{var}[\omega] = 2T^2 (G\sigma_{\Delta\gamma}^2)^2$ ;  $\sigma_{\omega T} = \sqrt{2} \cdot T \cdot G\sigma_{\Delta\gamma}^2$ .

Therefore, for  $G$  we have

$$G = \frac{\sigma_{\omega T}}{\sqrt{2} \cdot T \cdot \sigma_{\Delta\gamma}^2}. \quad (7)$$

If in  $T = 1000$  secs  $\sigma_{\omega T} = 1$  rad, assuming  $\sigma_{\Delta\gamma} = 1 \cdot 10^{-3}$ ,  $G \approx 7 \cdot 10^2$ .

In the simulation, the following model was assumed:

$$\begin{aligned} \Delta\gamma &\sim \mathcal{N}(0, \sigma_{\Delta\gamma}), \\ \sigma_{\Delta\gamma}(t) &= \sigma_{\Delta\gamma}(0) + h \cdot t, \\ \omega_i &= \omega_0 + G \cdot \Delta\gamma_i^2, \\ \phi_i &\sim \mathcal{N}(\phi_0, \sigma_\phi). \end{aligned}$$

Parameter	Value	Dimension
$\sigma_{\Delta\gamma}(0)$	$1 \cdot 10^{-3}$	
$h$	$5 \cdot 10^{-6}$	$1/sec$
$\omega_0$	3	$rad/sec$
$G$	$7 \cdot 10^2$	$rad/sec$
$\phi_0$	$\pi/2$	
$\sigma_\phi$	$2 \cdot 10^{-2}$	$rad$

### 2.2 Constant $\sigma_{\Delta\gamma}(t = 0)$

In order to have unchanging distributions of the beam particles' phase and oscillation frequency presented in Figure 1a we sampled  $\omega_i$ ,  $\phi_i$  once at  $t = 0$ , and only changed the time variable in eq. (1). The resulting polarization signal has the form shown in Figure 2.

One can observe (the detailization in Figure 2) that the black lines, marking the measurements supposed to be at the peaks/valleys of the signal (the null envelope), fall in front of the actual extrema after a while, which suggests that the signal's oscillation frequency is greater than that of the synchronous particle,  $\omega_0$ . With that in mind, we fitted the function  $f(t) = n_b \cdot \exp(\lambda t) \cdot \sin((\omega + g \cdot t) \cdot t + \phi_0)$  to the simulated data.

The model fit yielded an  $\hat{\omega} \approx 3.001 \pm 1.535 \cdot 10^{-6}$ , and a life-time  $\hat{\tau} \approx 2600$  sec. The frequency growth factor,  $g$ , is estimated  $g < 0$ , indicating a *decreasing* oscillation frequency. The estimate of  $g$  is statistically significant, with the t-value  $\approx -270$ ; we note, however, that the used model is drastically misspecified,<sup>1</sup> which might be the cause of the contradiction between the supposed deceleration of oscillation, and the evidence of the computed envelope points.

The signal's power spectrum (Figure 1b) mimics the particles'  $\omega$  density distribution.

### 2.3 Growing $\sigma_{\Delta\gamma}(t)$

In this simulation(Figure ), we resampled the  $(\omega, \phi)$  phase space at each measurement time. The effect of the growth of  $\sigma_{\Delta\gamma}$  can be observed not only in that the signal decays much more rapidly ( $\hat{\tau} \approx 454$  sec), but also in the increase of  $E[\hat{\omega}]$  from 3.001 to 3.002, caused by the appearance of a greater number of particles with higher frequencies.

<sup>1</sup>The first derivative of the signal's envelope falls much slower at the beginning.

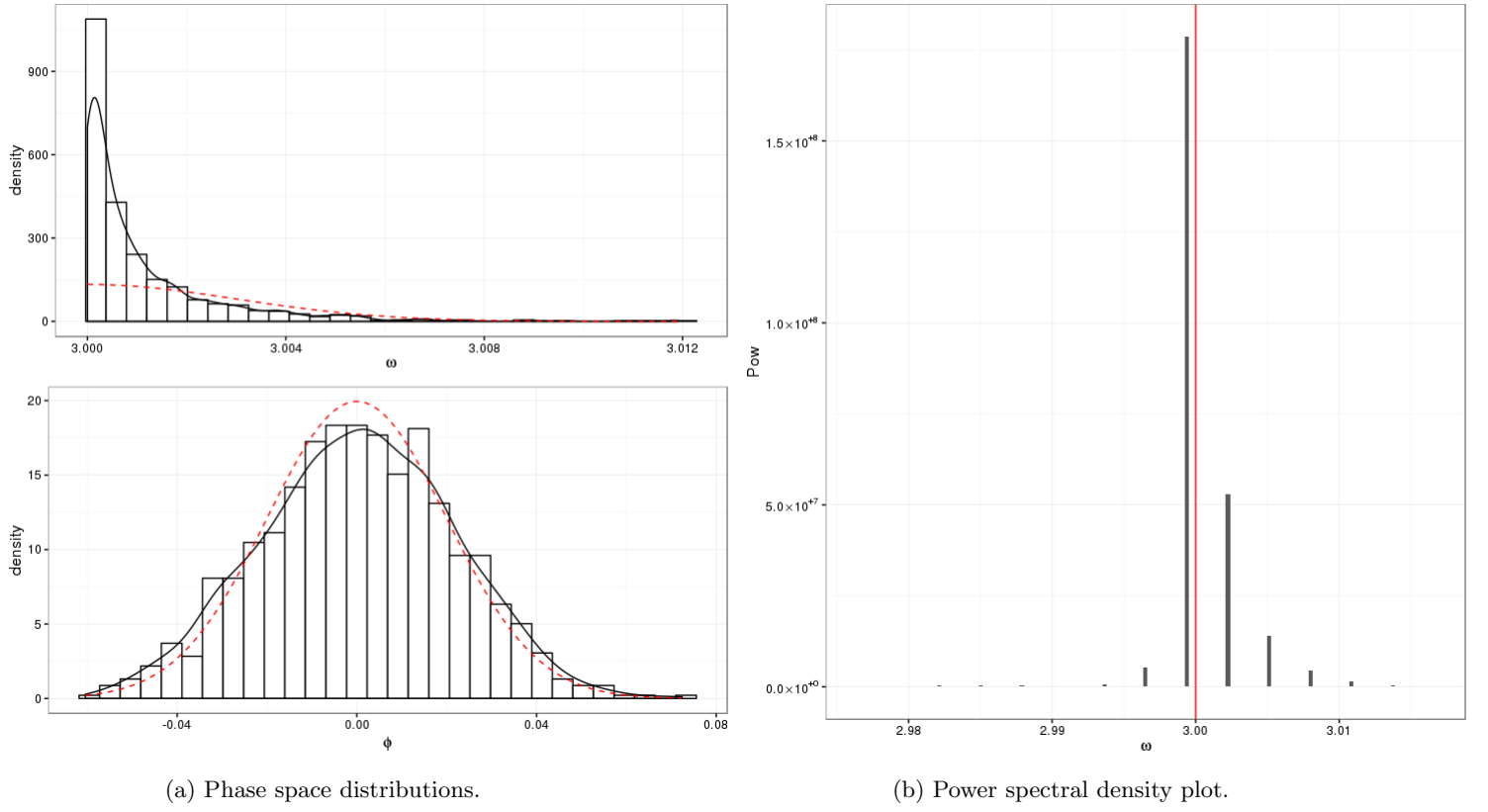


Figure 1: Distributions and power spectra.

## 2.4 Normally distributed $\omega$

The  $f_\omega, f_\phi$  distributions were kept constant throughout the simulation. In this case (Figure 4) the shift in the signal peaks from the null envelope is unnoticeable (as further evidenced by the non-convergence of the model with a frequency growth factor). Any systematic deviation of  $E[\hat{\omega}]$  is due to the asymmetry of the  $\omega$  distribution, and therefore decreases with the number of particles used in modeling.

## 3 Envelope

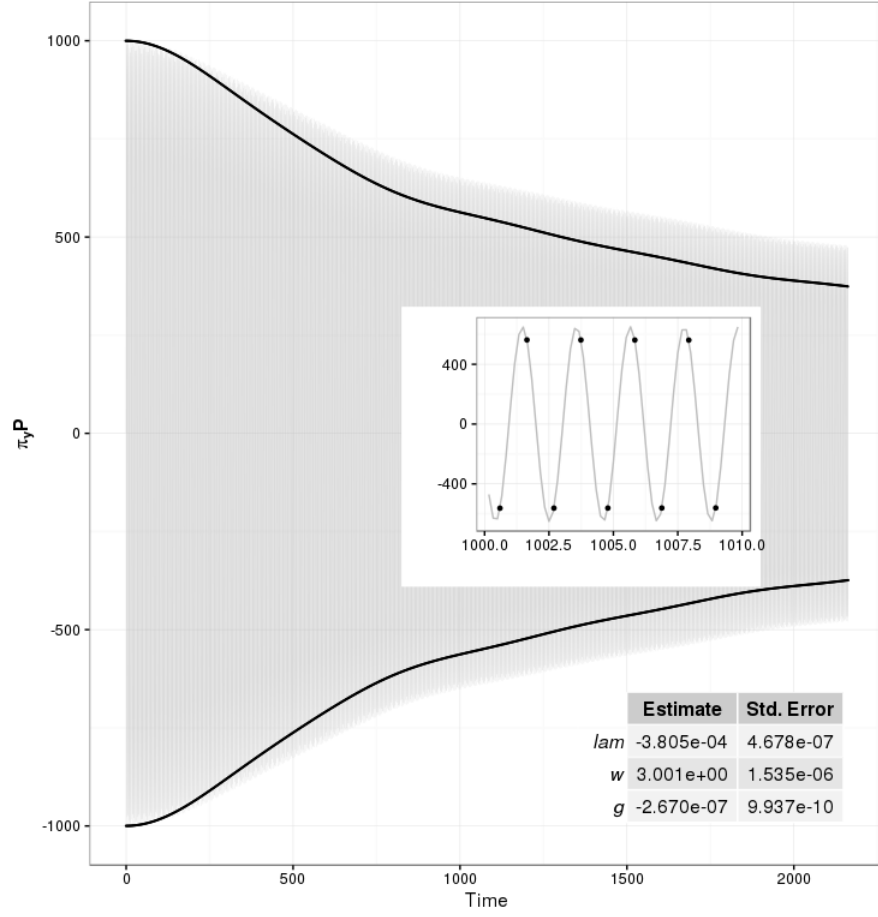


Figure 2: Polarization signal in the case of constant phase space distributions. The black lines mark the measurements taken at the points  $\sin(\omega_0 \cdot t_n + \phi_0) = \pm 1$ .

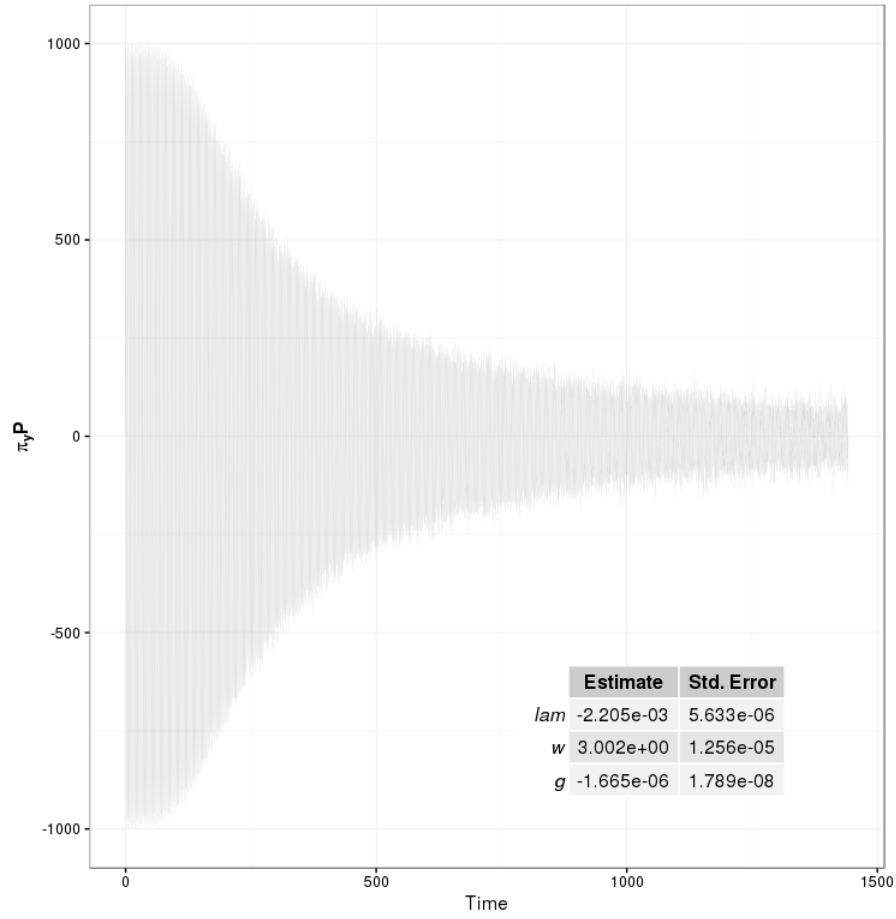
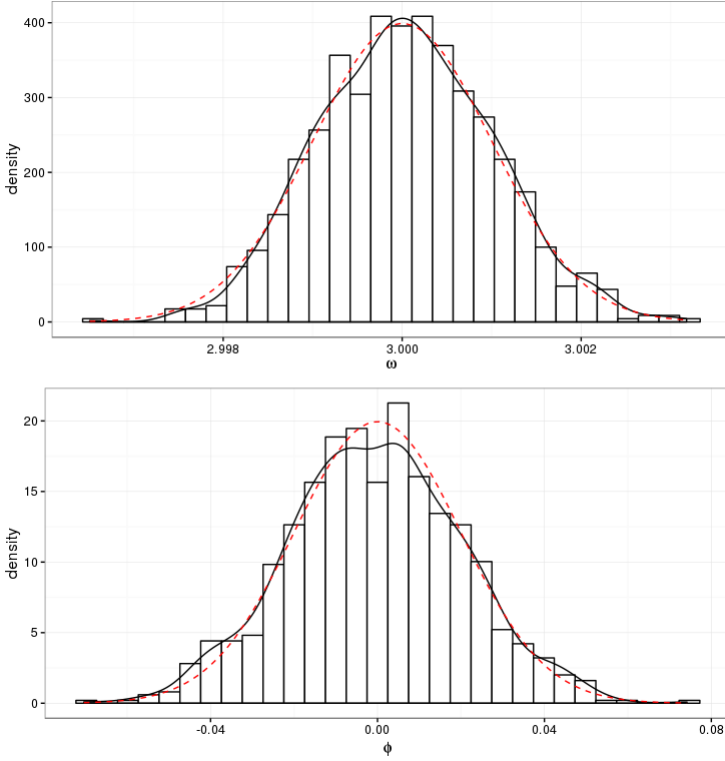
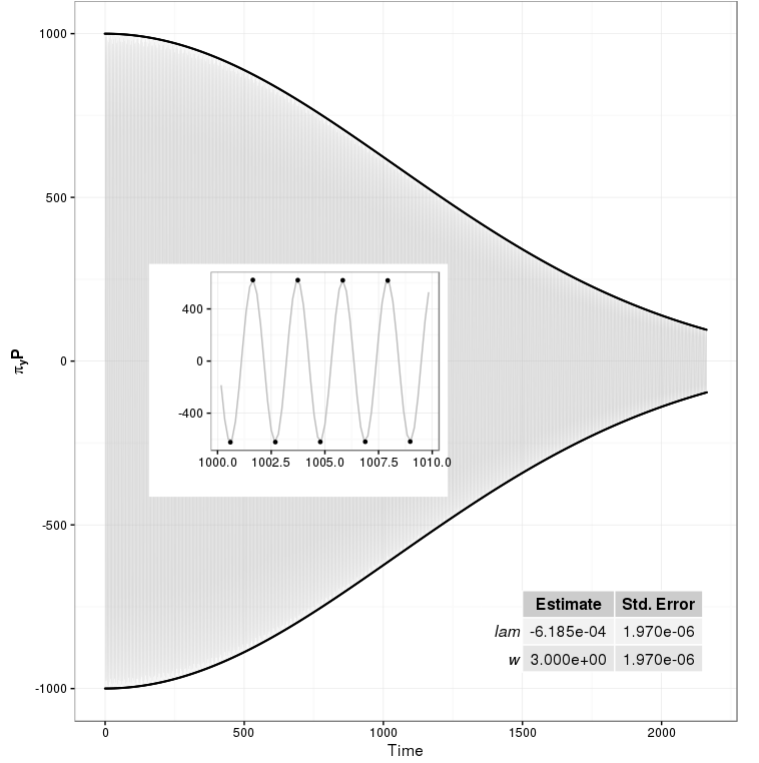


Figure 3: Decoherence when  $\sigma_{\Delta\gamma}$  grows with time.



(a) Phase space distributions.



(b) Signal in the case of a normally distributed oscillation frequency.

Figure 4: Normally distributed phase space variables.